(12)

AD-A187 401

DTIC FILE COPY

OFFICE OF NAVAL RESEARCH

Contract: N00014-85-K-0222

Work Unit: 4327-555

Scientific Officer: Dr. Richard S. Miller

Technical Report No. 11

CAVITATION IN MODEL ELASTOMERIC COMPOSITES

by

K. Cho and A. N. Gent

Institute of Polymer Science
The University of Akron
Akron, Ohio 44325

October, 1987

87 10 . 006

SECURITY CLASSIFICATION OF THIS PAGE (When Data Entered)

REPORT DOCUMENTATION PAGE		READ INSTRUCTIONS BEFORE COMPLETING FORM
1. REPORT NUMBER Technical Report No. 11	2. GOVT ACCESSION NO.	3. RECIPIENT'S CATALOG NUMBER
4. TITLE (and Subtitle) Cavitation in Model Elastomeric Composites		5. TYPE OF REPORT & PERIOD COVERED Technical Report
		6. PERFORMING ORG. REPORT NUMBER
7. AUTHOR(s) K. Cho and A. N. Gent		8. CONTRACT OR GRANT NUMBER(s) N00014-85-K-0222
9. PERFORMING ORGANIZATION NAME AND ADDRESS Institute of Polymer Science The University of Akron Akron, Ohio 44325		10. PROGRAM ELEMENT, PROJECT, TASK AREA & WORK UNIT NUMBERS 4327-555
11. CONTROLLING OFFICE NAME AND ADDRESS Office of Naval Research Power Program Arlington, VA 22217-5000		12. REPORT DATE October 1987
		13. NUMBER OF PAGES 29
14. MONITORING AGENCY NAME & ADDRESS(if different from Controlling Office)		15. SECURITY CLASS. (of this report) Unclassified
		15a. DECLASSIFICATION/DOWNGRADING SCHEDULE

16. DISTRIBUTION STATEMENT (of this Report)

According to attached distribution list.
Approved for public release; distribution unrestricted.

17. DISTRIBUTION STATEMENT (of the abstract entered in Block 20, if different from Report)

18. SUPPLEMENTARY NOTES

Submitted for publication in: Journal of Materials Science

19. KEY WORDS (Continue on reverse side if necessary and identify by block number)

Adhesion, Bonding, Cavitation, Composites, Elastomers, Fracture, Inclusions, Strength, Triaxial Stress

20. ABSTRACT (Continue on reverse side if necessary and identify by block number)

Layers of transparent silicone rubber were bonded between two steel spheres or between two parallel steel cylinders, to make simple mechanical models of particle-filled and fiber reinforced elastomers. When the steel end-pieces were pulled apart, visible cavities appeared suddenly in the rubber

layer between them, at well-defined tensile loads and displacements. The critical conditions for cavity formation are shown to be in good agreement with a theoretical criterion for the unbounded elastic expansion of a microscopic precursor void within the rubber: that the local triaxial tensile stress attains a value of 5E/6, where E is Young's modulus for the rubber. When the rubber layer was extremely thin, however, less than about 5 per cent of the steel endpiece diameter, then the stress required to form a cavity was greater than this, and it increased rapidly as the rubber thickness was reduced further. (Keywords)

1. Introduction

Composite materials show internal cracking when a sufficiently large stress is applied. In order to elucidate the mechanism of cracking, a number of studies have been carried out using simple models, in which a stiffer inclusion is incorporated into an elastic solid and the onset of failure near or at the surface of the inclusion is examined. Such studies have included thoria spheres embedded in a glass matrix (1), glass spheres embedded in a glassy polymer matrix (2,3), and glass and steel spheres embedded in a rubber matrix (4,5).

Variations in the strength of interfacial adhesion have been shown to affect not only the magnitude of the critical applied stress at which failure initiates, but also the nature of the failure itself (2,5). For a weakly-bonded rigid sphere in a rubber matrix, sudden detachment at the poles is observed when the applied stress reaches a sufficiently large value. On the other hand, when the rubber is well-bonded to the inclusion, a characteristic internal failure, termed cavitation, takes place near the poles of the inclusion, in the direction of the applied tension (4,5). This process consists of the sudden appearance of a void within the rubber itself, close to the surface of the inclusion but separated from it by a thin layer of still-attached rubber. It has been attributed to elastic expansion of a microscopic precursor void under the action of the local dilatant stress (negative hydrostatic pressure) $-P$ until the maximum extensibility of the material is exceeded and the void then grows to a visible size by tearing (6). This hypothetical mechanism of cavity formation in elastomers has been shown to account quantitatively for the appearance of cavities under triaxial tensions (6), under the action of dissolved supersaturated gases (7), and at points near spherical and rodlike inclusions where a sufficiently large triaxial tension is set up by an applied far-field tensile stress (4,5,8).

Unbounded elastic expansion of a spherical cavity in a rubber block is predicted to occur when the local dilatant stress exceeds a critical value, given by

$$-P_c = 5E/6 \tag{1}$$

where E is Young's modulus of the rubber (6). Good agreement is generally obtained with experimentally-observed conditions for the formation of visible cavities in soft rubbery solids.

One exception must be noted. When a rigid spherical inclusion is present, and is small in size, the critical far-field tensile stress for cavity formation is found to be considerably larger than that calculated from equation 1, and it increases steadily as the diameter of the inclusion is reduced (5). This anomaly is tentatively attributed to a second feature of the cavitation process: when the volume of material subjected to the dilatant stress is extremely small, say less than about 10^{-15}m^3, then the probability of finding a relatively large precursor void within it is also small. And when the precursor void is less than about 10^{-7}m in diameter, an additional restraint on its expansion becomes significant, arising from its own surface energy, so that cavitation becomes more difficult on this account (9).

We now turn to another aspect of internal void formation, and that is the effect of the close proximity of two inclusions upon the occurrence of voids between them. Cavities appear midway between two closely-spaced spherical inclusions lying in the direction of the applied tension (5), presumably when the dilatant stress set up there is sufficiently large. Simple models have therefore been constructed to represent highly-filled composites. They consist of two steel spheres or two parallel steel cylinders, bonded together with a layer of strongly-adhering transparent silicone rubber between them. They have been subjected to tensile forces in the direction of the two steel end-pieces, large enough to induce cavitation in the rubber phase. Results for the critical loads and deflections are reported here and compared with the predictions of equation 1, using a simple approximate solution for the dilatant stress set up in a layer of an incompressible elastic material bonded between two rigid spheres or two rigid parallel cylinders, when it is subjected to a tensile load in the direction of their centers.

2. Theoretical considerations

Values of the maximum hydrostatic tension $-P$ set up in the rubber layer can be obtained from an approximate stress analysis, assuming that the rubber is an incompressible, linearly-elastic solid. The results take the form (10),

$$-P_m/E = e_m/4A(A - 1)^2 \qquad (2)$$

for a layer bonded between two rigid spheres, Figure 1a, and

$$-P_m/E = e_m/2A(A - 1)^2 \qquad (3)$$

for a layer bonded between two parallel rigid cylinders, Figure 1b. The term A denotes

$$A = 1 + (h/D) \qquad (4)$$

where h is the separation distance of the spheres or cylinders and D is their diameter, and e_m is the maximum tensile strain set up in the rubber, given by the ratio of the displacement δ of one sphere or cylinder away from the other to the initial separation h: $e_m = \delta/h$.

The relations between e_m and the applied force F are somewhat complex; they are given in the original paper (10). However, they are not very different from the simple results:

$$e_m = \sigma/E \qquad (5)$$

for layers between spherical end-pieces, and,

$$e_m = 3\sigma/4E \qquad (6)$$

for layers between cylindrical end-pieces, where σ denotes the mean applied stress (10). With spherical end-pieces close together the observed and calculated strains e_m are somewhat larger than predicted by equation 5 and with closely-spaced cylindrical end-pieces they are smaller than predicted by equation 6, by a factor of up to 2X (10).

3. Experimental details

(i) Preparation of test-pieces.

Four sizes of steel balls were used to construct test-pieces having spherical end-pieces, Figure 1a. The diameters were 6.35 mm, 9.50 mm, 18.8 mm and 49.3 mm. Thin steel rods were welded to the outer poles of the balls tc hold them in a stretching device subsequently. Stainless steel tubes having an outer diameter of 9.55 mm, and of varied lengths in the range 12.5 mm to 50 mm, were used to construct test-pieces having cylindrical end-pieces, Figure 1b.

Surfaces of the steel balls and tubes were polished with fine emery paper and then coated with a special primer (Primer 92-023, Dow Corning Corporation) to give good adhesion to the silicone elastomer used. After the primer coating had dried, rubber layers were cast in the gap between two identical steel spheres or two identical cylinders using a mixture of 100 parts of Sylgard S-184 silicone polymer and 6 parts of Sylgard C-184 curing agent, both of which were obtained from

Dow Corning Corporation. The mixture was degassed under vacuum for 30 min and then poured into a mold surrounding the metal end-pieces and cured for 12 h at 120°C. Tensile measurements on a cured slab of the same formulation gave a value for Young's modulus E of 0.96 ± 0.05 MPa.

Specimens were prepared with various spacings h so that the ratio h/D ranged from about 0.02 up to about 0.35.

(ii) Measurement of applied forces or displacements at which cavitation occurred

Specimens with spherical end-pieces were stretched under an optical projector having a magnification of about 50X. The displacement δ at which a cavity was seen to appear suddenly in the rubber layer was measured directly in this way and employed using equation 2 to calculate the corresponding value of the hydrostatic tension $-P_m$.

Some experimentally-determined relations between tensile load, represented by the mean applied stress σ, and the corresponding displacement δ, are shown in Figure 2. They are seen to be approximately linear, up to maximum tensile strains of about 80 per cent, and values of the tensile stiffness K obtained from their slopes were in good agreement with those obtained previously for similar test-pieces subjected to small compressions (10). Thus, the assumption of linear elastic behavior appears to hold reasonably well for these specimens, even up to moderately high tensile strains.

For specimens with cylindrical end-pieces, the critical loads at which a visible cavity suddenly appeared were measured directly using a tensile test apparatus. The specimens were stretched at a rate of about 10 μm s^{-1}, until a cavity appeared, and the corresponding displacements were then calculated from the measured critical loads using theoretical stiffness values for such test-pieces (10). The corresponding values of hydrostatic tension $-P_m$ were obtained from equation 3.

It should be noted that only stresses arising from the restraints at the bonded surfaces are considered in this procedure for determining the triaxial tensile stress $-P_m$; simple tensile stresses are neglected. They should be relatively small, however, for specimens with closely-spaced end-pieces.

4. Experimental results

(i) Formation of cavities

Photographs of representative cavities are shown in Figures 3 and 4, for specimens with spherical and cylindrical end-pieces, respectively. The cavities appeared suddenly when the critical load was reached and grew rapidly to a large size. They formed in the general area of maximum tensile strain and maximum hydrostatic tension, sometimes near one of the end-pieces, Figure 3, and sometimes midway between them, Figure 4. Similar observations were reported previously for a rubber block containing two spherical inclusions (5).

It was noticed that the formation of cavities was somewhat time-dependent; that is, when a load slightly smaller than the value taken here to be the critical one was applied and maintained for several seconds, a cavity would often appear in the same way as in steadily-increasing loading. This feature is tentatively ascribed to time dependence of the tensile modulus and tear strength of the silicone rubber used.

(ii) Conditions for cavitation

Values of the critical dilatant stress $\underline{-P_m}$ for cavity formation, determined as described above from the measured critical loads or displacements, are given in Tables 1 and 2 for specimens with spherical and cylindrical end-pieces, respectively. They are also plotted in Figures 5 and 6 against the ratio $\underline{h/D}$ of the end-piece separation to diameter of the sphere or cylinder. The horizontal broken lines in each of these Figures represent the theoretically-predicted result, equation 1.

Experimental results for rubber layer thicknesses greater than about 5 per cent of the end-piece diameter are seen to be in reasonably good agreement with the theoretical cavitation stress for a highly elastic solid containing a precursor void. This is the case for layers bonded to either spherical or cylindrical end-pieces and for a wide range of end-piece diameters. As the relations for dilatant stress are rather different in these two cases, equations 2 and 3, the general agreement found to hold strongly suggests that the observed cavities arise from the proposed mechanism of unstable elastic expansion of precursor voids under the action of a critical dilatant stress.

At extremely small thicknesses of the rubber layer, less than about 5 per cent of the end-piece diameter, the stresses necessary to form a large cavity became considerably greater than those for thicker rubber layers, Figure 5, as much as four times greater when the layer thickness was only about 2 per cent of the end-piece diameter. This feature was found to hold for specimens with spherical end-pieces having a wide range of diameter, suggesting that it was not simply a function of the layer thickness itself but of the ratio of thickness to end-piece diameter. It is reminiscent of the previous observation that cavitation is more difficult to bring about near small spherical inclusions (5). Once again, it appears that an additional restraint on cavity formation is operative in small volumes of rubber near highly-curved surfaces, in addition to the simple elastic resistance that governs the process in larger samples.

5. Conclusions

Large cavities have been found to form in layers of rubber bonded between rigid spheres or cylinders when the assembly is put into tension. The critical tensile loads and deflections are in generally good agreement with a simple fracture criterion: that a critical level of the local dilatant stress $-P$, of about $5E/6$, is reached. This is the theoretical value at which unbounded elastic expansion of a (hypothetical) precursor void would take place. Thus, it appears that visible cavities occur as a result of such a process, and form when and where the critical dilatant stress level is attained. However, when the rubber layer is extremely thin, less than about 5 per cent of the end-piece diameter, then cavitation requires substantially higher stresses. For a regular arrangement of spheres on a cubic lattice, this close proximity corresponds to a high volume concentration of filler particles, of more than 45 per cent.

Acknowledgements

This work forms part of a program of research on highly-filled elastomeric composites supported by the Office of Naval Research (Contract N00014-85-K-0222). A grant-in-aid from Lord Corporation is also gratefully acknowledged.

References

1. R. W. Davidge and T. J. Green, J. Mater. Sci. 3 (1968) 629.

2. M. E. J. Dekkers and D. Heikens, J. Mater. Sci. 18 (1983) 3281.

3. M. E. J. Dekkers and D. Heikens, J. Mater. Sci. 20 (1985) 3873.

4. A. E. Oberth, Rubb. Chem. Technol. 40 (1967) 1337.

5. A. N. Gent and B. Park, J. Mater. Sci. 19 (1984) 1947.

6. A. N. Gent and P. B. Lindley, Proc. Roy. Soc. (Lond.) A249 (1959) 195.

7. A. N. Gent and D. A. Tompkins, J. Appl. Phys. 40 (1969) 2520.

8. K. Cho, A. N. Gent and P. S. Lam, J. Mater. Sci., in press.

9. A. N. Gent and D. A. Tompkins, J. Polym. Sci., Part A-2 7 (1969) 1483.

10. A. N. Gent and B. Park, Rubb. Chem. Technol. 59 (1986) 77.

Table 1: Effect of separation distance h on the cavitation strain e_m and dilatant stress $-P_m$ for specimens with spherical end-pieces of diameter D.

D(mm)	h(mm)	h/D	δ(mm)	e_m	$-P_m/E$
6.34	0.95	0.150	0.87	0.92	1.33
	1.33	0.210	1.52	1.14	1.12
	1.93	0.304	1.95	1.01	0.64
9.51	0.19	0.020	0.05	0.26	3.22
	0.22	0.023	0.06	0.27	2.91
	0.37	0.039	0.07	0.19	1.16
	0.38	0.040	0.11	0.29	1.74
	0.43	0.045	0.10	0.23	1.24
	0.74	0.078	0.25	0.34	1.00
18.80	0.27	0.014	0.04	0.15	2.68
	0.73	0.039	0.22	0.30	1.85
49.30	0.69	0.014	0.14	0.20	3.58
	0.84	0.017	0.21	0.25	3.50
	2.51	0.051	0.76	0.30	1.40
	2.93	0.058	1.02	0.35	1.46
	16.96	0.335	18.32	1.08	0.62

Table 2. Effect of separation distance h on the cavitation strain e_m and dilatant stress $-P_m$ for specimens with cylindrical end-pieces of diameter D = 9.55 mm.

Length L (mm)	h (mm)	h/D	F (N)	[illegible] (mm)[a]	e_m[a]	$-P_m/E$[b]
12.5	0.43	0.045	25	0.034	0.08	0.84
	0.91	0.095	66	0.255	0.28	1.35
	1.21	0.127	77	0.440	0.36	1.27
25.5	1.00	0.105	114	0.161	0.161	0.70
	1.36	0.142	122	0.395	0.29	0.90
	1.51	0.158	127	0.476	0.32	0.86
50.0	0.85	0.089	170	0.150	0.18	0.91
	0.95	0.099	206	0.209	0.22	1.02
	1.16	0.121	212	0.286	0.25	0.90
	1.24	0.130	216	0.317	0.26	0.87

a: Calculated from F.

b: Calculated from e_m using equation 3.

Figure Captions

Figure 1: (a) Rubber layer (cross-hatched) bonded between two steel spheres.

(b) Rubber layer (cross-hatched) bonded between two parallel steel tubes.

Figure 2: Experimental relations between mean tensile stress σ and ratio e of displacement δ to initial separation h for rubber layers bonded between two steel spheres.

Figure 3: Cavity formed in a silicone rubber layer bonded between two steel spheres at a tensile strain e_m = 0.23. Initial separation h = 0.43 mm, diameter D = 9.50 mm.

Figure 4: Cavity formed in a silicone rubber layer bonded between two steel cylinders at a tensile strain e_m = 0.08. Initial separation h = 0.43 mm, diameter D = 9.55 mm.

Figure 5: Dilatant stress $-P_m$ for cavity formation in a silicone rubber layer bonded between two steel spheres *vs* ratio h/D of initial separation distance h to sphere diameter D. D = 6.35 mm, ● ; 9.5 mm, ◒ ; 18.8 mm, ○ ; 49.3 mm, ◑ . The horizontal broken line represents the predicted result from equation 1.

Figure 6: Dilatant stress $-P_m$ for cavity formation in a silicone rubber layer bonded between two parallel steel cylinders *vs* ratio h/D of initial separation distance h to cylinder diameter D. D = 9.55 mm, L = 12.5 mm, ● ; 25.5 mm, ○ ; 50 mm, ◒ . The horizontal broken line represents the predicted result from equation 1.

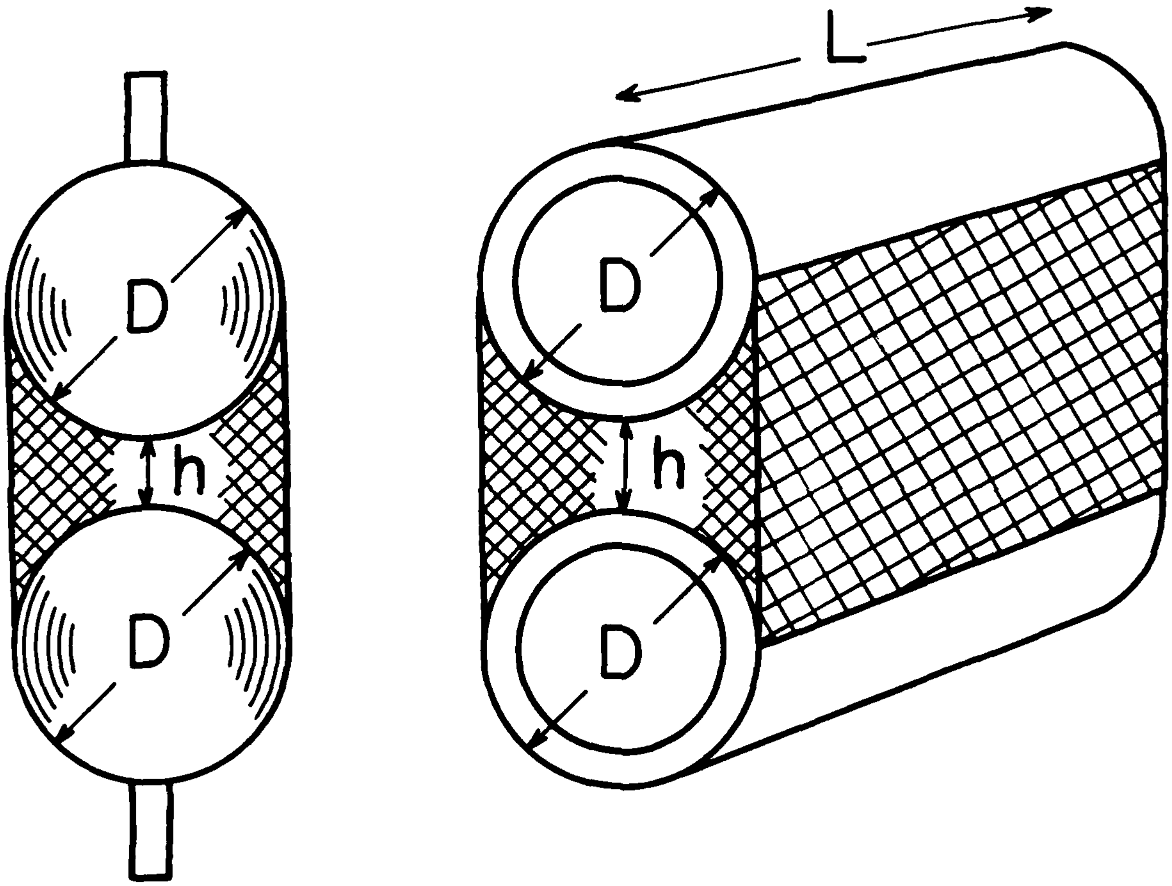

(a) (b)

FIGURE 1

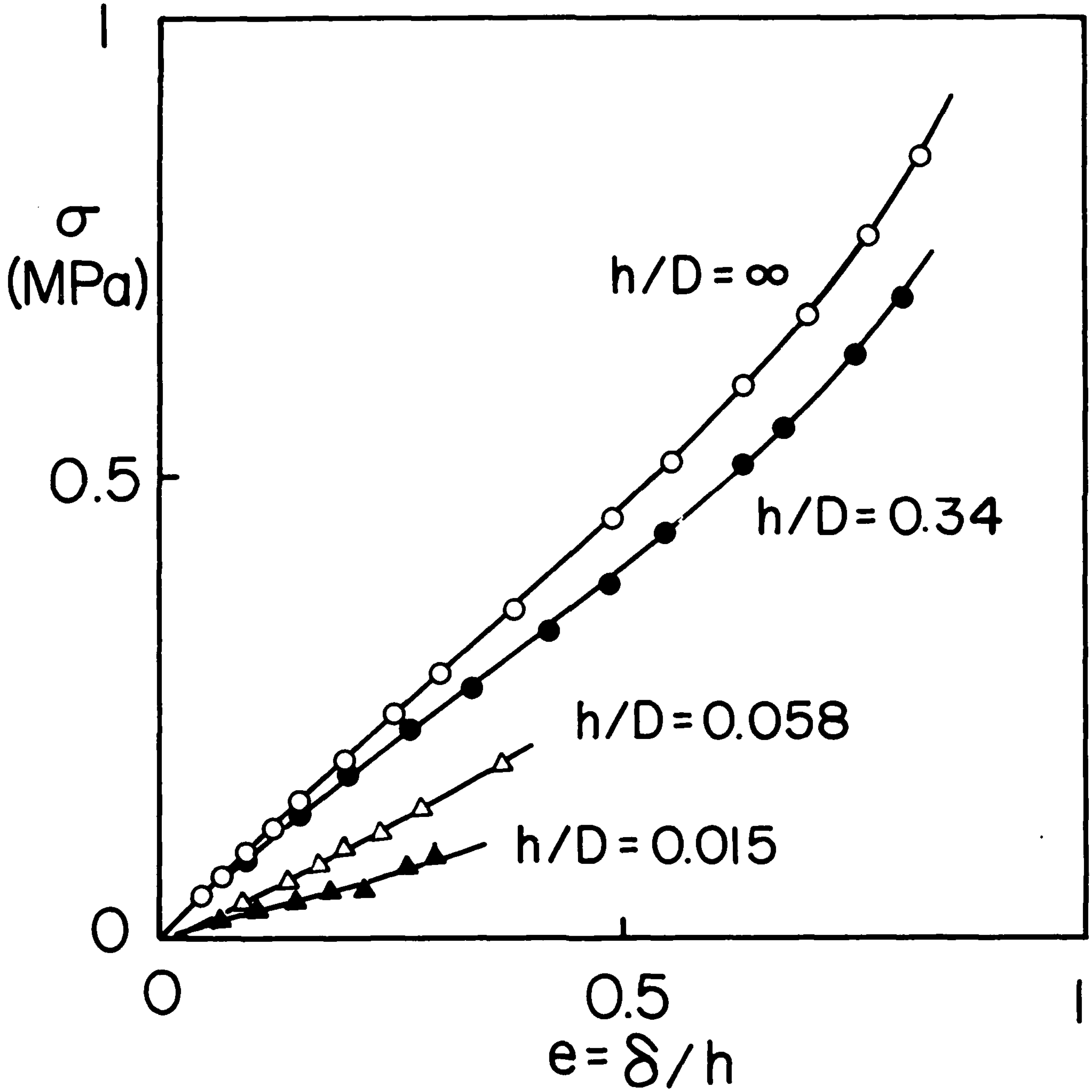

FIGURE 2

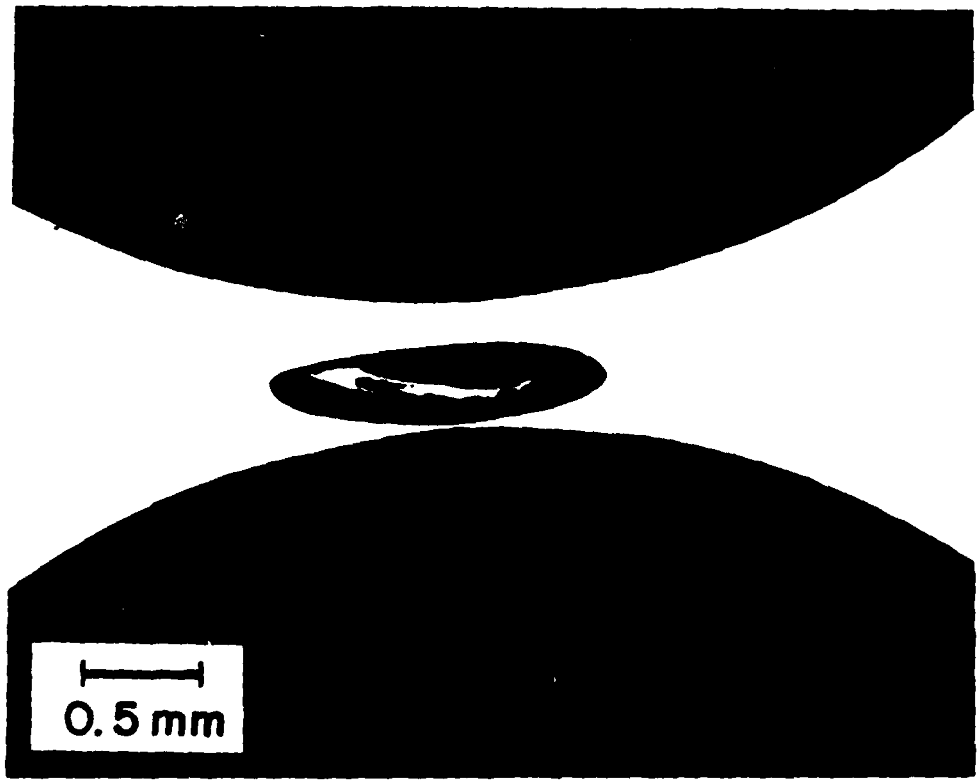

FIGURE 3

FIGURE 4

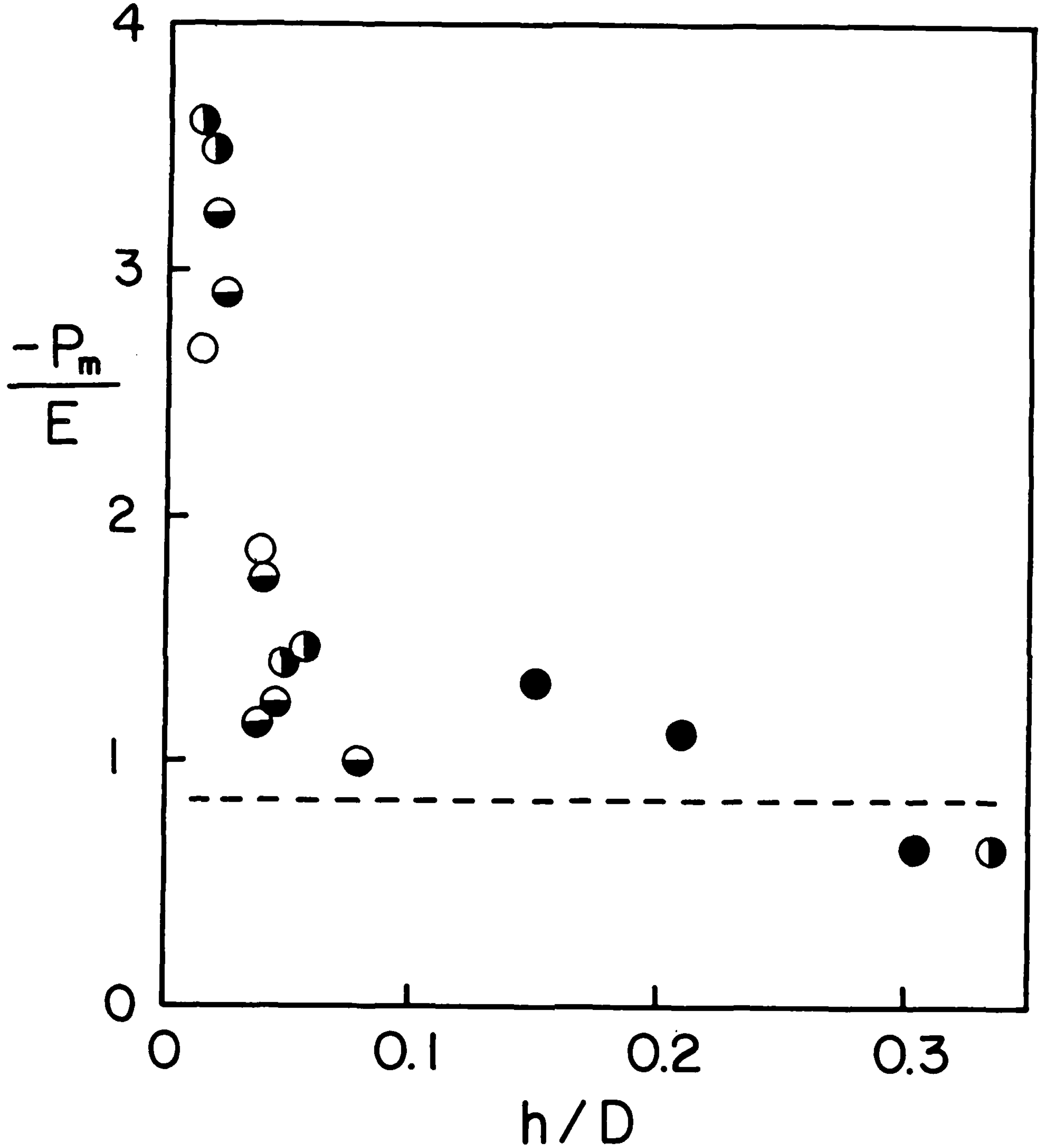

FIGURE 5

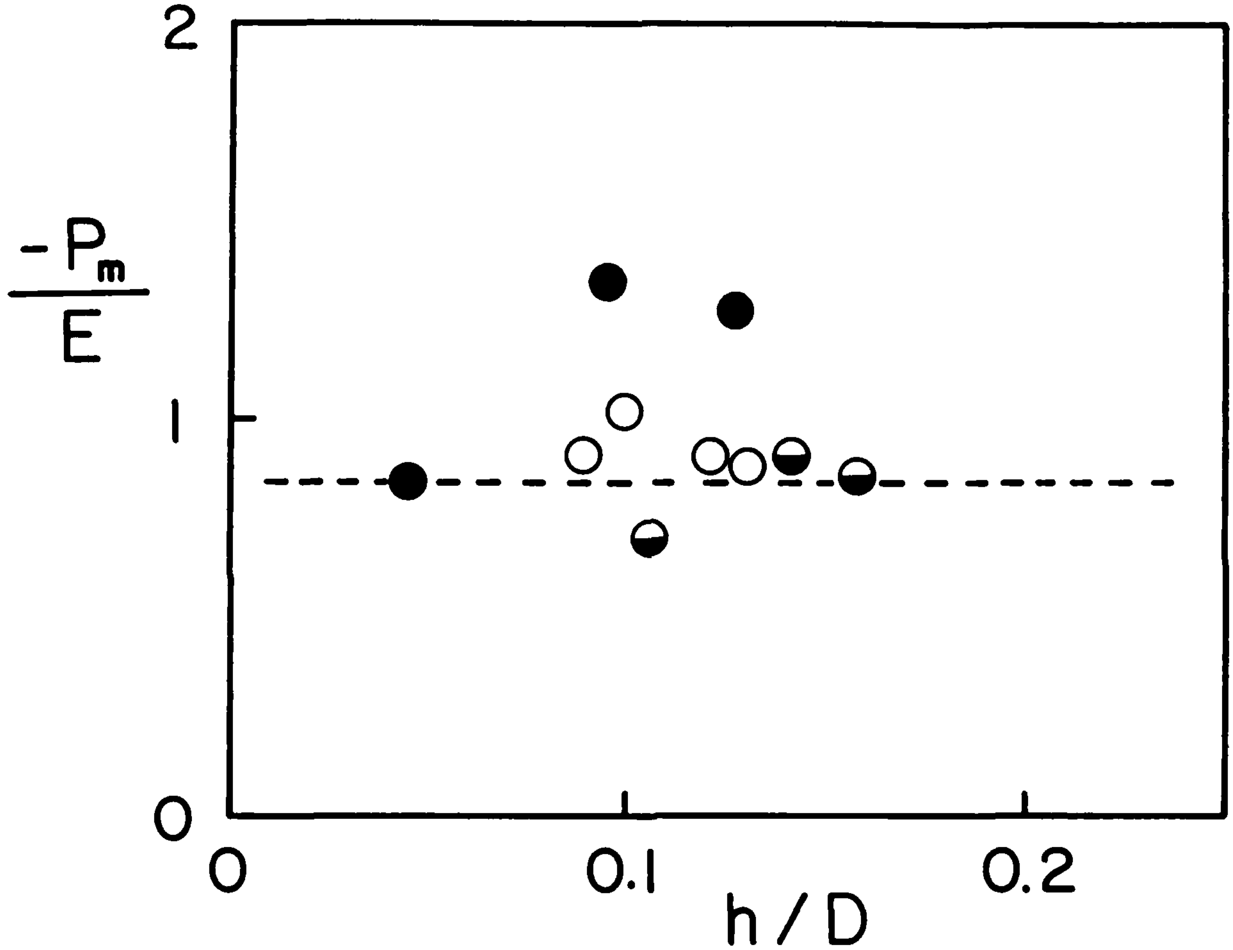

FIGURE 6

(DYN)

DISTRIBUTION LIST

Dr. R.S. Miller
Office of Naval Research
Code 432P
Arlington, VA 22217
(10 copies)

Dr. J. Pastine
Naval Sea Systems Command
Code 06R
Washington, DC 20362

Dr. Kenneth D. Hartman
Hercules Aerospace Division
Hercules Incorporated
Alleghany Ballistic Lab
P.O. Box 210
Washington, DC 21502

Mr. Otto K. Heiney
AFATL-DLJG
Elgin AFB, FL 32542

Dr. Merrill K. King
Atlantic Research Corp.
5390 Cherokee Avenue
Alexandria, VA 22312

Dr. R.L. Lou
Aerojet Strategic Propulsion Co.
Bldg. 05025 - Dept 5400 - MS 167
P.O. Box 15699C
Sacramenta, CA 95813

Dr. R. Olsen
Aerojet Strategic Propulsion Co.
Bldg. 05025 - Dept 5400 - MS 167
P.O. Box 15699C
Sacramento, CA 95813

Dr. Randy Peters
Aerojet Strategic Propulsion Co.
Bldg. 05025 - Dept 5400 - MS 167
P.O. Box 15699C
Sacramento, CA 95813

Dr. D. Mann
U.S. Army Research Office
Engineering Division
Box 12211
Research Triangle Park, NC 27709-2211

Dr. L.V. Schmidt
Office of Naval Technology
Code 07CT
Arlington, VA 22217

JHU Applied Physics Laboratory
ATTN: CPIA (Mr. T.W. Christian)
Johns Hopkins Rd.
Laurel, MD 20707

Dr. R. McGuire
Lawrence Livermore Laboratory
University of California
Code L-324
Livermore, CA 94550

P.A. Miller
736 Leavenworth Street, #6
San Francisco, CA 94109

Dr. W. Moniz
Naval Research Lab.
Code 6120
Washington, DC 20375

Dr. K.F. Mueller
Naval Surface Weapons Center
Code R11
White Oak
Silver Spring, MD 20910

Prof. M. Nicol
Dept. of Chemistry & Biochemistry
University of California
Los Angeles, CA 90024

Mr. L. Roslund
Naval Surface Weapons Center
Code R10C
White Oak, Silver Spring, MD 20910

Dr. David C. Sayles
Ballistic Missile Defense
Advanced Technology Center
P.O. Box 1500
Huntsville, AL 35807

(DYN)

DISTRIBUTION LIST

Mr. R. Geisler
ATTN: DY/MS-24
AFRPL
Edwards AFB, CA 93523

Naval Air Systems Command
ATTN: Mr. Bertram P. Sobers
NAVAIR-320G
Jefferson Plaza 1, RM 472
Washington, DC 20361

R.B. Steele
Aerojet Strategic Propulsion Co.
P.O. Box 15699C
Sacramento, CA 95813

Mr. M. Stosz
Naval Surface Weapons Center
Code R10B
White Oak
Silver Spring, MD 20910

Mr. E.S. Sutton
Thiokol Corporation
Elkton Division
P.O. Box 241
Elkton, MD 21921

Dr. Grant Thompson
Morton Thiokol, Inc.
Wasatch Division
MS 240 P.O. Box 524
Brigham City, UT 84302

Dr. R.S. Valentini
United Technologies Chemical Systems
P.O. Box 50015
San Jose, CA 95150-0015

Dr. R.F. Walker
Chief, Energetic Materials Division
DRSMC-LCE (D), B-3022
USA ARDC
Dover, NJ 07801

Dr. Janet Wall
Code 012
Director, Research Administration
Naval Postgraduate School
Monterey, CA 93943

Director
US Army Ballistic Research Lab.
ATTN: DRXBR-IBD
Aberdeen Proving Ground, MD 21005

Commander
US Army Missile Command
ATTN: DRSMI-RKL
Walter W. Wharton
Redstone Arsenal, AL 35898

Dr. Ingo W. May
Army Ballistic Research Lab.
ARRADCOM
Code DRXBR - 1BD
Aberdeen Proving Ground, MD 21005

Dr. E. Zimet
Office of Naval Technology
Code 071
Arlington, VA 22217

Dr. Ronald L. Derr
Naval Weapons Center
Code 389
China Lake, CA 93555

T. Boggs
Naval Weapons Center
Code 389
China Lake, CA 93555

Lee C. Estabrook, P.E.
Morton Thiokol, Inc.
P.O. Box 30058
Shreveport, Louisiana 71130

Dr. J.R. West
Morton Thiokol, Inc.
P.O. Box 30058
Shreveport, Louisiana 71130

Dr. D.D. Dillehay
Morton Thiokol, Inc.
Longhorn Division
Marshall, TX 75670

G.T. Bowman
Atlantic Research Corp.
7511 Wellington Road
Gainesville, VA 22065

(DYN)

DISTRIBUTION LIST

R.E. Shenton
Atlantic Research Corp.
7511 Wellington Road
Gainesville, VA 22065

Mike Barnes
Atlantic Research Corp.
7511 Wellington Road
Gainesville, VA 22065

Dr. Lionel Dickinson
Naval Explosive Ordinance
Disposal Tech. Center
Code D
Indian Head, MD 20340

Prof. J.T. Dickinson
Washington State University
Dept. of Physics 4
Pullman, WA 99164-2814

M.H. Miles
Dept. of Physics
Washington State University
Pullman, WA 99164-2814

Dr. T.F. Davidson
Vice President, Technical
Morton Thiokol, Inc.
Aerospace Group
110 North Wacker Drive
Chicago, Illinois 60606

Mr. J. Consaga
Naval Surface Weapons Center
Code R-16
Indian Head, MD 20640

Naval Sea Systems Command
ATTN: Mr. Charles M. Christensen
NAVSEA-62R2
Crystal Plaza, Bldg. 6, Rm 806
Washington, DC 20362

Mr. R. Beauregard
Naval Sea Systems Command
SEA 64E
Washington, DC 20362

Brian Wheatley
Atlantic Research Corp.
7511 Wellington Road
Gainesville, VA 22065

Mr. G. Edwards
Naval Sea Systems Command
Code 62R32
Washington, DC 20362

C. Dickinson
Naval Surface Weapons Center
White Oak, Code R-13
Silver Spring, MD 20910

Prof. John Deutch
MIT
Department of Chemistry
Cambridge, MA 02139

Dr. E.H. deButts
Hercules Aerospace Co.
P.O. Box 27408
Salt Lake City, UT 84127

David A. Flanigan
Director, Advanced Technology
Morton Thiokol, Inc.
Aerospace Group
110 North Wacker Drive
Chicago, Illinois 60606

Dr. L.H. Caveny
Air Force Office of Scientific Research
Directorate of Aerospace Sciences
Bolling Air Force Base
Washington, DC 20332

W.G. Roger
Code 5253
Naval Ordance Station
Indian Head, MD 20640

Dr. Donald L. Ball
Air Force Office of Scientific Research
Directorate of Chemical & Atmospheric Sciences
Bolling Air Force Base
Washington, DC 20332

(DYN)

DISTRIBUTION LIST

Dr. Anthony J. Matuszko
Air Force Office of Scientific Research
Directorate of Chemical & Atmospheric Sciences
Bolling Air Force Base
Washington, DC 20332

Dr. Michael Chaykovsky
Naval Surface Weapons Center
Code R11
White Oak
Silver Spring, MD 20910

J.J. Rocchio
USA Ballistic Research Lab.
Aberdeen Proving Ground, MD 21005-5066

G.A. Zimmerman
Aerojet Tactical Systems
P.O. Box 13400
Sacramento, CA 95813

B. Swanson
INC-4 MS C-346
Los Alamos National Laboratory
Los Alamos, New Mexico 87545

Dr. James T. Bryant
Naval Weapons Center
Code 3205B
China Lake, CA 93555

Dr. L. Rothstein
Assistant Director
Naval Explosives Dev. Engineering Dept.
Naval Weapons Station
Yorktown, VA 23691

Dr. M.J. Kamlet
Naval Surface Weapons Center
Code R11
White Oak, Silver Spring, MD 20910

Dr. Henry Webster, III
Manager, Chemical Sciences Branch
ATTN: Code 5063
Crane, IN 47522

Dr. A.L. Slafkosky
Scientific Advisor
Commandant of the Marine Corps
Code RD-1
Washington, DC 20380

Dr. H.G. Adolph
Naval Surface Weapons Center
Code R11
White Oak
Silver Spring, MD 20910

U.S. Army Research Office
Chemical & Biological Sciences Division
P.O. Box 12211
Research Triangle Park, NC 27709

G. Butcher
Hercules, Inc.
MS X2H
P.O. Box 98
Magna, Utah 84044

W. Waesche
Atlantic Research Corp.
7511 Wellington Road
Gainesville, VA 22065

Dr. John S. Wilkes, Jr.
FJSRL/NC
USAF Academy, CO 80840

Dr. H. Rosenwasser
AIR-320R
Naval Air Systems Command
Washington, DC 20361

Dr. Joyce J. Kaufman
The Johns Hopkins University
Department of Chemistry
Baltimore, MD 21218

Dr. A. Nielsen
Naval Weapons Center
Code 385
China Lake, CA 93555

(DYN)

DISTRIBUTION LIST

K.D. Pae
High Pressure Materials Research Lab.
Rutgers University
P.O. Box 909
Piscataway, NJ 08854

Dr. John K. Dienes
T-3, B216
Los Alamos National Lab.
P.O. Box 1663
Los Alamos, NM 87544

A.N. Gent
Institute Polymer Science
University of Akron
Akron, OH 44325

Dr. D.A. Shockey
SRI International
333 Ravenswood Ave.
Menlo Park, CA 94025

Dr. R.B. Kruse
Morton Thiokol, Inc.
Huntsville Division
Huntsville, AL 35807-7501

G. Butcher
Hercules, Inc.
P.O. Box 98
Magna, UT 84044

W. Waesche
Atlantic Research Corp.
7511 Wellington Road
Gainesville, VA 22065

Dr. R. Bernecker
Naval Surface Weapons Center
Code R13
White Oak
Silver Spring, MD 20910

Prof. Edward Price
Georgia Institute of Tech.
School of Aerospace Engineering
Atlanta, GA 30332

J.A. Birkett
Naval Ordnance Station
Code 5253K
Indian Head, MD 20640

Prof. R.W. Armstrong
University of Maryland
Dept. of Mechanical Engineering
College Park, MD 20742

Herb Richter
Code 38[illegible]
Naval Weapons Center
China Lake, CA 93555

J.T. Rosenberg
SRI International
333 Ravenswood Ave.
Menlo Park, CA 94025

G.A. Zimmerman
Aeroject Tactical Systems
P.O. Box 13400
Sacramento, CA 95813

Prof. Kenneth Kuo
Pennsylvania State University
Dept. of Mechanical Engineering
University Park, PA 16802

T.L. Boggs
Naval Weapons Center
Code 3891
China Lake, CA 93555

(DYN)

DISTRIBUTION LIST

Dr. C.S. Coffey
Naval Surface Weapons Center
Code R13
White Oak
Silver Spring, MD 20910

D. Curran
SRI International
333 Ravenswood Avenue
Menlo Park, CA 94025

E.L. Throckmorton
Code SP-2731
Strategic Systems Program Office
Crystal Mall #3, RM 1048
Washington, DC 23076

Dr. R. Martinson
Lockheed Missiles and Space Co.
Research and Development
3251 Hanover Street
Palo Alto, CA 94304

C. Gotzmer
Naval Surface Weapons Center
Code R-11
White Oak
Silver Spring, MD 20910

G.A. Lo
3251 Hanover Street
B204 Lockheed Palo Alto Research Lab
Palto Alto, CA 94304

R.A. Schapery
Civil Engineering Department
Texas A&M University
College Station, TX 77843

J.M. Culver
Strategic Systems Projects Office
SSPO/SP-2731
Crystal Mall #3, RM 1048
Washington, DC 20376

Prof. G.D. Duvall
Washington State University
Department of Physics
Pullman, WA 99163

Dr. E. Martin
Naval Weapons Center
Code 3858
China Lake, CA 93555

Dr. M. Farber
135 W. Maple Avenue
Monnovia, CA 91016

W.L. Elban
Naval Surface Weapons Center
White Oak, Bldg. 343
Silver Spring, MD 20910

G.E. Manser
Morton Thickol
Wasatch Division
P.O. Box 524
Brigham City, UT 84302

R.G. Rosemeier
Brimrose Corporation
7720 Belair Road
Baltimore, MD 20742

Administrative Contracting
Officer (see contract for
address)
(1 copy)

Director
Naval Research Laboratory
Attn: Code 2627
Washington, DC 20375
(6 copies)

Defense Technical Information Center
Bldg. 5, Cameron Station
Alexandria, VA 22314
(12 copies)

Dr. Robert Polvani
National Bureau of Standards
Metallurgy Division
Washington, D.C. 20234

Dr. Y. Gupta
Washington State University
Department of Physics
Pullman, WA 99163